

Glacial-interglacial seawater isotope change near the Chilean Margin as reflected by $\delta^2\text{H}$ values of C₃₇ alkenones.

Katrin Hättig¹, Devika Varma¹, Stefan Schouten^{1,2}, Marcel T. J. van der Meer¹

¹ Department of Marine Microbiology and Biogeochemistry, NIOZ Royal Netherlands Institute for Sea Research, Texel, the Netherlands

² Department of Earth Sciences, Faculty of Geosciences, Utrecht University, Utrecht, the Netherlands

Correspondence to: Katrin Hättig (katrin.haettig@nioz.nl)

Abstract. Stable hHydrogen isotopic compositions of long-chain alkenones with 37 carbon atoms ($\delta^2\text{H}_{\text{C}37}$) have been shown to reflect~~proposed as a proxy for past~~ seawater salinity in culture and environmental studies and this potential sea surface salinity proxy has been applied to in several down core records from different regions. However, previous studies were based solely on a single sediment core and often suggested unlikely large changes in salinity based on existing proxy calibrations. Here we present a new $\delta^2\text{H}_{\text{C}37}$ record, in combination with oxygen isotopes of benthic foraminifera from the same samples, from a sediment core from the Chilean Margin (ODP site 1235). The observed negative shift in $\delta^2\text{H}_{\text{C}37}$ of 20‰ during the last deglaciation was identical to that of a previously published $\delta^2\text{H}_{\text{C}37}$ record from the nearby located, but deeper, ODP core 1234, suggesting a regionally consistent shift in $\delta^2\text{H}_{\text{C}37}$. This change~~shift~~ translates into a negative hydrogen isotope shift of the surface seawater of ca. 14‰, similar to glacial–interglacial reconstructions based on other $\delta^2\text{H}_{\text{C}37}$ records. The reconstructed bottom seawater oxygen isotope change based on benthic foraminifera during the last deglaciation is approximately -0.8‰, in line with previous studies. When translated into hydrogen isotopes of bottom sea water using the modern open-ocean water line, this would suggest a negative change~~shift~~ of ca. 5‰, smaller than the reconstructed surface seawater shift based on alkenones. The larger~~higher~~ change in surface~~surface~~ water isotopes suggests that it experienced more freshening during the Holocene than bottom waters, either due to increased freshwater input or reduced evaporation, or a combination of the two.

1 Introduction

The stable oxygen and hydrogen isotope~~ie~~ composition of seawater ($\delta^{18}\text{O}_{\text{sw}}$ and $\delta^2\text{H}_{\text{sw}}$, respectively) reveals crucial information about (sea)water physicochemical properties, which could improve~~s~~ our understanding of past global ocean current dynamics and changes therein. Several oceanographic factors can cause shifts in the isotopic composition of seawater: for example, the bottom seawater isotopic composition depends on the source area of the water and reflects the history of advection associated transport, mixing, upwelling and downwelling of ocean currents (Rohling and Cooke, 1999). Regional factors affecting the sea–surface seawater isotopic composition are the evaporation–precipitation balance, river water input, iceberg melting, and the local climate regime (Rohling and Cooke, 1999). On a more global level, land ice formation is an important process which~~that~~ affects oxygen and hydrogen isotopes of seawater, where~~–~~ during glacial periods large amounts

of water with relatively low $\delta^{18}\text{O}$ and $\delta^2\text{H}$ oxygen and hydrogen isotope values are stored as ice on land, increasing seawater $\delta^{18}\text{O}$ values leaving the more enriched in the heavier isotopes (e.g. Schrag et al., 2002). Decreasing global ice volume during warmer interglacials, releases this fresh, low-density water with relatively low $\delta^{18}\text{O}$ and $\delta^2\text{H}$ values into the surface ocean. During warmer interglacials, the decrease in global ice volume leads to the formation of low density fresh water with relatively low $\delta^{18}\text{O}$ and $\delta^2\text{H}$ values which enters the surface ocean (Rohling and Bigg, 1998). Since both evaporation and precipitation affect sea-water isotopes and salinity increase as a result of evaporation and decrease as a result of precipitation or freshwater input in a similar way, seawater isotopes and salinity are tightly coupled have a close relationship with the salinity of the ocean (Rohling 2007; Craig 1961; Craig and Gordon 1965). Therefore, sea-water isotopes are often reconstructed and used to infer past salinity changes (e.g. Lamy et al., 2002; Schrag et al., 2002; Rousselle et al., 2013).

There are several methods available to reconstruct the isotopic composition of sea-water. The stable oxygen isotopic composition of foraminifera ($\delta^{18}\text{O}_{\text{foram}}$) is a function of the oxygen isotope composition of ambient sea water ($\delta^{18}\text{O}_{\text{sw}}$) and calcification temperature (Bemis et al., 1998; Epstein et al., 1953; Shackleton, 1974) with a minor effect of carbonate ion concentration (Spero et al., 1997). Temperature-corrected $\delta^{18}\text{O}_{\text{foram}}$ is thus assumed to reflect $\delta^{18}\text{O}_{\text{sw}}$, though with some uncertainty (Duplessy et al., 1991; Rostek et al., 1993). Generally, temperature corrections of $\delta^{18}\text{O}_{\text{foram}}$ to reconstruct $\delta^{18}\text{O}_{\text{sw}}$ are done based on temperature proxies derived from the same foraminifera, such as Mg/Ca (e.g. Billups et al., 2002, 2003; Lear et al., 2000, 2004, 2015; Martin et al., 2002) or carbonate clumped isotopes (Δ_{47}) (e.g. Petersen et al., 2015). In some cases, independent temperature proxies based on organic geochemical indices, such as U^{238}_{37} and TEX_{86} (Brassell et al., 1986; Prahl et al., 1987; Schouten et al., 2003), are used to correct for the temperature (Rostek et al., 1993, 1997). Several studies based on $\delta^{18}\text{O}_{\text{foram}}$ -records, $\delta^{18}\text{O}$ values of porewaters and modelling, estimate a negative global average change of 0.8–1.1‰ in the oxygen isotope ratio of the global sea-water during the last deglaciation (e.g. Adkins and Schrag et al., 2001; Adkins et al., 2002; Duplessy et al., 2002; Oba et al., 2004; Waelbroeck et al., 2002). Based on this, the salinity change is thought to be around 1–2 psu (Adkins et al., 2002; Broecker, 2002). Deriving To derive salinity from local $\delta^{18}\text{O}_{\text{sw}}$ estimates, i.e. those corrected for global $\delta^{18}\text{O}_{\text{sw}}$ changes, requires knowledge of the regional relationship between $\delta^{18}\text{O}_{\text{sw}}$ and salinity the salt content (LeGrande and Schmidt, 2006; Rohling, 2007). However, it is uncertain whether this relationship is consistent through time was similar in the past as it is today.

The hydrogen isotopic composition of sea-water is more difficult to reconstruct. Schrag et al. (2002) One way is to measured the hydrogen isotopic composition of pore fluids in deep-sea sediments and showed. Those indicate a negative shift change of 6–9‰ in the hydrogen isotopic $\delta^2\text{H}_{\text{sw}}$ composition of the bottom sea water ($\delta^2\text{H}_{\text{BSW}}$) during the last glacial to interglacial transition change. Another potential proxy for reconstructing surface sea water ($\delta^2\text{H}_{\text{SSW}}$) is based on the combined hydrogen isotopic composition of long-chain alkenones combined $\text{C}_{37.2}$ and $\text{C}_{37.3}$ alkenones ($\delta^2\text{H}_{\text{C37}}$) with 37 carbon atoms and two and three double bonds $\delta^2\text{H}_{\text{C37}}$ derived from haptophyte algae, produced by haptophyte algae. Culture studies show that the hydrogen isotopic fractionation of phototrophic organisms depends not only on the hydrogen isotopic composition of sea-water but also on salinity (M'Boule et al., 2014; Sachs et al., 2016; Schouten et al., 2006; Weiss et al., 2017a; Zhang et al., 2009; Zhang et al., 2007). However, the response of $\delta^2\text{H}_{\text{C37}}$ to salinity varies significantly between haptophyte species (M'Boule et

65 a., 2014; Sachs et al., 2016; Schouten et al., 2006), as well as in ~~the environmental settings where sometimes no impact of salinity on $\delta^2\text{H}_{\text{C}37}$ is found~~ (Gould et al., 2019; Häggi et al., 2015; Mitsunaga et al., 2022; Weiss et al., 2019b). ~~These differences or absences in response of $\delta^2\text{H}$ to salinity makes quantitatively constraining past salinity changes difficult. The application of $\delta^2\text{H}_{\text{C}37}$ to sediment cores Downcore records~~ show a ~~decrease~~ shift of 16–25‰ in $\delta^2\text{H}_{\text{C}37}$ (when corrected for ice volume 9–18‰) for the last deglaciation ~~to Recent~~ depending on the site (Kasper et al., 2014; Pahnke et al., 2007; Petrick et al., 2015; Simon et al., 2015; Weiss et al., 2019a). ~~Based on these results, Weiss et al. (2019b) reconstructed glacial–interglacial salinity changes of 5–19 psu, based on multiple different $\delta^2\text{H}_{\text{C}37}$ –salinity calibrations. These reconstructed glacial–interglacial salinity changes are much larger than based on $\delta^{18}\text{O}$ and ice volume modelling (e.g. Oba et al., 2004; Adkins et al., 2002). This large glacial interglacial shift in $\delta^2\text{H}_{\text{C}37}$ suggests large salinity changes (5 to 19 psu) when using culture and especially core top calibrations, much larger than expected.~~ Therefore, Weiss et al. (2019b) concluded ~~that either glacial–interglacial salinity changes are larger than previously assumed or the a higher~~ paleo sensitivity of $\delta^2\text{H}_{\text{C}37}$ to salinity changes ~~was higher in the past~~ than observed in modern-day environments and cultures.

70 A different approach ~~would be to directly is to~~ correlate $\delta^2\text{H}_{\text{C}37}$ ~~with $\delta^2\text{H}_{\text{SSW}}$ rather than salinity~~. Gould et al. (2019) observed a statistically significant $\delta^2\text{H}_{\text{C}37}$ – ~~$\delta^2\text{H}_{\text{SSW}}$~~ relationship with open-ocean suspended particulate organic matter (SPOM)–~~and~~ and Mitsunaga et al. (2022) showed a statistically identical relationship based on core top sediments. This suggests that in the 80 natural environment, the effects of factors like salinity, species composition (e.g. Chivall et al., 2014; M'Boule et al., 2014), ~~and~~ light and nutrients (Sachs et al., 2015; van der Meer et al., 2015) on stable hydrogen isotope fractionation during biosynthesis may be less important than the isotopic composition of sea-water. This observation allows direct inference of $\delta^2\text{H}_{\text{SSW}}$ from $\delta^2\text{H}_{\text{C}37}$ without any additional correction, though this approach has not been applied yet to reconstruct past $\delta^2\text{H}_{\text{SSW}}$. Mitsunaga et al. (2022) did ~~predict suggest~~ a “global” LGM–Modern change of ~~–~~12.7‰ in the hydrogen isotopic composition 85 of alkenones ~~based on the global $\delta^{18}\text{O}_{\text{SW}}$ shift, a waterline slope of 8 and their core top calibration, based on several assumptions~~. Similar ~~as forte~~ $\delta^{18}\text{O}_{\text{SW}}$, reconstructed $\delta^2\text{H}_{\text{SSW}}$ can then be converted into salinity using modern-day correlations between surface $\delta^2\text{H}_{\text{SSW}}$ and salinity (LeGrande and Schmidt, 2006; Rohling, 2007).

90 ~~Here, we generated a $\delta^2\text{H}_{\text{C}37}$ and benthic $\delta^{18}\text{O}_{\text{foram}}$ record of ODP core 1235 from the Chilean Margin (Fig. 1) and compared this with the previously published hydrogen isotope (Weiss et al., 2019b) and temperature records (de Bar et al., 2018) from nearby ODP core 1234. Both cores are which is only ~12 km away from each other, though at a much greater different water depths (489 m versus 1015 m), and are expected to record the same surface seawater signal (Mix et al., 2003). Furthermore, in In contrast to Weiss et al. (2019b), we reconstructed $\delta^2\text{H}$ values of surface seawater and compared this to bottom seawater oxygen isotopes values ($\delta^{18}\text{O}_{\text{BSW}}$) inferred from measured benthic foraminifera $\delta^{18}\text{O}$ values and used both to constrain relative salinity change during the deglaciation.~~

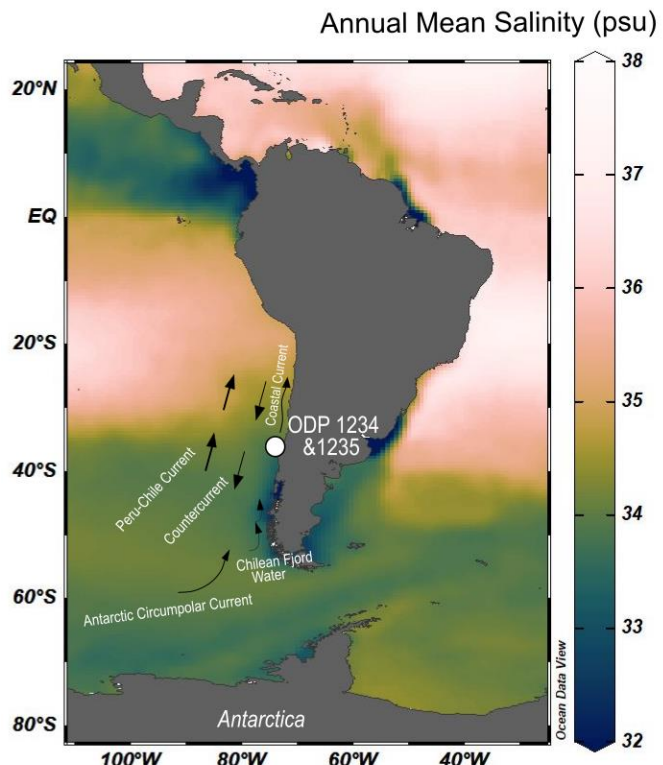


Figure 1: Map of sea surface salinity (data from Zweng et al., 2018, scientific colour map from Crameri et al., 2022) showing the sediment core locations of the neighbouring cores ODP 1234 and ODP 1235. The core location is influenced by ~~three~~^{two} primary ocean currents: the Northward Peru-Chile Current and the Chilean Coastal Current, as well as the southward Peru-Chile Countercurrent. Those are fed by the Antarctic Circumpolar waters, and Chilean Fjord waters can also enter from the southeast the system.

100 2 Material and Methods

2.1 Geographic Setting

The ODP site 202-1235 was ~~retrieved drilled~~ at 36.16°S, 73.57°W at a ~~relatively~~ shallow water depth of 489 m (Fig. 1). The site is about 12 km away from the deeper-located neighbouring ODP 202-1234 site (36.22°S, 73.68°W, water depth 1015 m) in the southeast Pacific Ocean (Mix et al., 2003) (Fig. 1). These sites are located ~~at~~ on the Chilean Margin which is influenced by surface and deep-water currents which cause upwelling, stimulating local productivity (Bakun, 1989). The setting is dynamic with south-westerly winds and freshwater runoff from the continent. The Antarctic Circumpolar Current (ACC) transports cold and saline water into the Peru-Chile Countercurrent which could be mixed with fresher fjord water, with a lower $\delta^2\text{H}$ value, along the southern margin is feeding into the Peru-Chile Countercurrent and transports cold saline waters. Isotopically depleted water can potentially be added by the Chilean Fjord water which feeds the Chile Coastal Current (Lamy

110 et al., 2002; Strub et al., 1998; De Baret al., 2018). The present-day annual mean sea surface salinity in the study area is 33.8 ±0.2 psu ([World Ocean Atlas 2018, 0.25deg grid](#): Zweng et al., 2018).

2.2 Sampling and age model

Sediment samples of core ODP 1235 were split into two subsamples: Approximately 6 g of wet sediment was used for foraminiferal oxygen isotope analysis ($\delta^{18}\text{O}_{\text{foram}}$) and approximately 10 g of wet sediment was used for organic proxy analysis, i.e., $U_{37}^{K'}$, TEX₈₆ (see Varma et al., [2023, under revision](#)) and $\delta^{2}\text{H}_{\text{C37}}$ (this study). Samples were taken every 5–10 cm to cover a resolution of <2 ka, and a total of 27 samples were analysed for hydrogen isotopes.

The age-depth models for ~~ODP 1234 and ODP 1235 and the neighbouring ODP core 1234~~ were both constructed with the statistical package Bacon (Blaauw and Christeny, 2011) using a Bayesian approach and are based on the radiocarbon ages of mixed benthic foraminifera (Muratli et al., 2010; this study, Table S1) as outlined by Varma et al. (2023). ODP 1234 has a mean sedimentation rate of 20 cm ka⁻¹ and ODP 1235 a rate of 5 cm ka⁻¹. ~~Additionally, three radiocarbon measurements from benthic foraminifera species *Uvigerina* from ODP 1235 were performed using the Mini Carbon Dating System (MICADAS) at the Alfred Wegener Institute (AWI; Table S1). The oldest tie point for both cores is the Laschamp event at 41 000 years, based on magnetic susceptibility correlation between the cores ODP 1233, ODP 1234 and ODP 1235 (Mix et al., 2003; Table S1). Since the latter tie point of 41 ka, with 51 meters and 27 meters composite depth for ODP 1235 and 1234, respectively, is a rough estimation (Mix et al., 2003), the data points in the records between 3040 ka likely have an uncertainty of around ±1 ka assuming a constant sedimentation rate. Radiocarbon ages were converted into calendar years using Marine09 data set (Reimer et al., 2009) with the reservoir correction given by (Muratli et al., 2010). The core chronology was constructed with the statistical package Bacon (Blaauw and Christeny, 2011) using a Bayesian approach. ODP 1234 has a mean sedimentation rate of 20 cm ka⁻¹ and ODP 1235 a rate of 5 cm ka⁻¹.~~

130 2.3 Analysis of benthic foraminifera and long-chain alkenones

Stable oxygen isotopes were measured on the benthic foraminifera species *Uvigerina* with an automated carbonate device (Kiel IV, Thermo Scientific) connected to a Thermo Finnigan MAT 253 dual inlet isotope ratio mass spectrometer. The sample sizes were ca. 20 µg and contained 2–5 foraminifera shells (>150 µm). Replicate analyses of $\delta^{18}\text{O}$ values of the same sample had a standard deviation of ~~were averaged with average differences being~~ 0.016–0.2‰. NBS 19 limestone was used as the isotope calibration standard, and for drift detection and correction, a second standard, NFHS-1, was used. For both standards ~~t~~he standard deviation is within 0.1‰ for $\delta^{18}\text{O}$. All carbonate isotope data are given in per mill (‰) relative to V-PDB (Vienna – Pee Dee Belemnite). Calculated $\delta^{18}\text{O}$ seawater values are given in per mill (‰) relative to V-SMOW (Vienna – Standard Mean Ocean Water) with the accepted conversion value of 0.27‰ (Hut, 1987; Pearson, 2012).

The sediment split for organic analysis was extracted as described by Varma et al. (2023). Briefly, sediments were first freeze-dried and then extracted using an Dionex 350 Accelerated Solvent Extractor. The solvent from the total extract was first

removed using a Turbovap and the last remaining water, if present, was removed using a small sodium sulfate column to obtain the total lipid extract (TLEs). The TLEs were separated into three fractions over a small alumina column (Al_2O_3) column using hexane/ dichloromethane 9:1 (v:v) to elute first the apolar fraction, hexane/ DCM 1:1 (v:v) to elute the ketone (alkenone) fraction, and dichloromethane/ methanol 1:1 (v:v) to elute the polar fraction. The ketone fractions were used for compound-specific hydrogen isotope ratio measurements of alkenones, after being measured using a gas chromatograph coupled to a flame ionization detector (GC-FID) to determine the correct concentration and complexity of the fraction. Hydrogen isotope ratios were measured in duplicate using a gas chromatograph coupled to a Thermo Delta V isotope ratio mass spectrometer via high-temperature conversion reactor (Isolink I) and Conflo IV. The GC was equipped with an RTX-200 60 m column following Weiss et al. (2019). We report the hydrogen isotope ratio, relative to V-SMOW, of the individual alkenones $\text{C}_{37:3}$ and $\text{C}_{37:2}$ and the integrated $\text{C}_{37} \delta^2\text{H}$ ratios determined by manual peak integration of the combined $\text{C}_{37:3}$ and $\text{C}_{37:2}$ peaks (van der Meer et al., 2013). The H_{3+} factor was measured daily ~~before~~ prior to running samples and shifted in time never more than 0.5 ppm/nA per day. ~~The performance and stability of the instrument was monitored by measuring an n-alkane mixture standard, Mix B (A. Schimmelmann, Indiana University) at the start of each day. The performance and stability of the instrument were monitored by measuring a standard containing 15 n-alkanes at different concentrations (Mix B from A. Schimmelmann, Indiana University), at the start of each day. Samples were only run when the average difference between the measured values for the Mix B standard and the certified values for this standard and their standard deviation were less than 5%. Samples were only run when the average difference and standard deviation between values was less than 5%.~~ With each sample, squalene and a C_{30} n-alkane were co-injected to monitor the system performance. ~~Their measured values with measured values ranging from of~~ $-173 \pm 5\text{‰}$ and $-78 \pm 4\text{‰}$. ~~The fit well with their offline pre~~ determined values are of $-170 \pm 4\text{‰}$ for squalene and $-79 \pm 5\text{‰}$ for the C_{30} n-alkane.

2.4 Modern open-ocean isotopic composition of sea-water

The relationship between $\delta^{18}\text{O}$ - $\delta^2\text{H}$ in the water-atmosphere environment can be described with the meteoric water-line (MWL) and is close to $\delta^2\text{H} = 8 \times \delta^{18}\text{O} + 10$ according to Craig (1961) and Craig et al. (1965). To describe the relationship in surface ocean waters and investigate the potential for palaeoceanographic applications, Rohling (2007) correlated measured $\delta^{18}\text{O}$ and $\delta^2\text{H}$ of sampled ~~surface~~ ocean waters ~~(top 250 m)~~. We updated the dataset of Rohling (2007) with data from the Waterisotope Database (2022) managed by Dr. G. Bowen (University of Utah) and published data from Gould et al. (2019), Weiss et al. (2019a) and Srivastava et al. (2010) (Fig. S2, S3). This extended seawater isotope dataset contains 1550 datapoints ~~from all water depths, not limited to the top 250 or 300 m, from the open-ocean, with the following fit and a root mean square error () of 3‰:~~

$$170 \quad \delta^2\text{H}_{\text{SW}} = 6.58 (\pm 0.07) \times \delta^{18}\text{O}_{\text{SW}} - 0.12 (\pm 0.03) \quad (R^2 = 0.82; \text{RMSE} = 3\text{‰}) \quad (1)$$

We will refer to this correlation as modern open-ocean water line (MOOWL). The relationship between the hydrogen isotopic composition of the surface seawater and the measured salinity in the modern open-ocean is based on the top 300 m water depth, 424903 datapoints are obtained from the extended seawater isotope dataset:

$$\delta^2H_{SW} = 3.53 (\pm 0.10) \times S - 122.57 (\pm 3.52) \quad (R^2 = 0.66; \text{RMSE} = 0.8 \text{ psu}) \quad (2)$$

175 Finally, the oxygen isotopic composition of the surface seawater (top 300 m) and the salinity were correlated based on 5602 datapoints:

$$\delta^{18}O_{SW} = 0.52 (\pm 0.01) \times S - 18.02 (\pm 0.18) \quad (R^2 = 0.64; \text{RMSE} = 0.8 \text{ psu}) \quad (3)$$

2.5 Calculation of Past Seawater Isotopes

2.5.1 Bottom Seawater

180 The oxygen isotopic composition of foraminifera ($\delta^{18}O$) depends mainly on the temperature of calcification (T) and isotope ratio of the water. ($\delta^{18}O_{SW}$) McCrea (1950) published the first laboratory oxygen-isotope paleotemperature equation which was subsequently revised and extended to different calcite polymorphs and foraminifera species (e.g. Bemis et al., 1998; Cramer et al., 2011; Epstein et al., 1953; Lynch-Stieglitz et al., 1999; Mulitza et al., 2003; O'Neil et al., 1969; Shackleton, 1974; Spero et al., 2003). The relationship can be described as the following, where d is the slope and c is the intercept:

$$185 \quad T = c + d \times (\delta^{18}O_{foram} - \delta^{18}O_{SW}) \quad (4)$$

This relationship is used, in combination with temperature proxies, to reconstruct past $\delta^{18}O_{SW}$ values using temperature proxies and, subsequently, obtain salinity estimations using the $\delta^{18}O_{SW}$ – salinity relationship (Lamy et al., 2002; Pearson, 2012; Tang and Stott, 1993; Ganssen et al., 2011). The most relevant paleotemperature equation for benthic foraminifera is currently from Lynch-Stieglitz et al. (1999), adjusted to V-SMOW by Cramer et al. (2011), where The $\delta^{18}O$ -paleotemperature relationship 190 is estimated with the in field calibration of in situ benthic foraminifera from the genera *Cibicidoides* and *Planulina* (Lynch-Stieglitz et al., 1999). *Uvigerina* genera $\delta^{18}O$ values are corrected to *Cibicidoides* and *Planulina* $\delta^{18}O$ values Recent studies adjust data of other genera to fit with those (e.g. Cramer et al., 2009, 2011). We adjusted the oxygen isotope ratios of *Uvigerina* in this study by 0.64‰ to fit with *Cibicidoides* and *Planulina* $\delta^{18}O$ values (i.e., Shackleton, 1974), these can be used, for the $\delta^{18}O_{BSW}$ reconstruction. Important to note is that $\delta^{18}O_{SW}$ is always measured on the V-SMOW scale, whereas calcite is 195 standardized to V-PDB. The accepted value to convert V-PDB into V-SMOW at the time of Eq. (5) (Cramer et al., 2011) is 0.27‰.

$$T = 16.1 - 4.76 * (\delta^{18}O_{foram} - (\delta^{18}O_{BSW} - 0.27)) \quad (5)$$

Rearranged to $\delta^{18}O_{BSW}$:

$$\delta^{18}O_{BSW} = \frac{-16.1 + 4.76 \times \delta^{18}O_{foram} + T}{4.76} + 0.27 \quad (6)$$

To estimate the surface δ^2H_{SSW} signal from the measured hydrogen isotopic composition of alkenones, we used the suspended organic matter calibration (SPOM) from Gould et al. (2019, reduced dataset):

$$\delta^2H_{C37} = 1.48 (\pm 0.4) \times \delta^2H_{\text{SSW}} - 199 (\pm 3) \quad (R^2 = 0.2; \text{RSME} = 5.8\%) \quad (7)$$

The environmental δ^2H_{C37} – δ^2H_{SSW} calibration from Gould et al. (2019) is based on alkenones from mainly open-ocean Group III haptophytes living in the Atlantic and Pacific ocean, covering large environmental differences such as salinity, temperature, nutrient concentrations and light intensity that in turn affect growth rate, for instance. We calculated a root mean square error (RMSE) of 5.8‰ for this calibration using the reduced data set of Gould et al. (2019).

An alternative environmental calibration is the sediment core –top study from Mitsunaga et al. (2022), where they extended and revised the data of Weiss et al. (2019a):

210

$$\delta^2H_{C37} = 1.44 (\pm 0.13) \times \delta^2H_{\text{SSW}} - 191.62 (\pm 1.13) \quad (R^2 = 0.61; \text{RSME} = 7\%) \quad (8)$$

3 Results and Discussion

3.1 Reconstruction of bottom seawater isotopes based on foraminifera

The oxygen isotopes $\delta^{18}\text{O}$ values of benthic *Uvigerina* in ODP core 1235 ranges between 4.15‰ to 2.27‰ (Fig. 1). Between 215 40 to 27 ka, the $\delta^{18}\text{O}_{\text{foram}}$ is relatively stable with values between 3.13 to 3.96‰, followed by a decrease towards a value of 2.27‰ at 25 ka. Between 25 and 20 ka, the $\delta^{18}\text{O}_{\text{foram}}$ signal is more positive/higher with values of 3.7 – 4.15‰ and rapidly shifts by 1.6‰ to all values of 2.27‰ in the uppermost sample. This record is consistent with ODP core 1234, showing a negative isotope shift from the n LGM to 1 ka shift of ca. 1.7‰ in the $\delta^{18}\text{O}$ values of *Uvigerina* (de Bar et al., 2018).

To reconstruct $\delta^{18}\text{O}_{\text{BSW}}$, we need to reconstruct bottom water temperatures, which unfortunately, we were not able to do. To 220 obtain some indications of temperature change, we used published SST records from the same core. The organic SST proxy $U_{37}^{K'}$ measured in this core (from Varma et al., 2023) indicates a temperature range of 11.9 °C to 16.9 °C, with relatively stable temperatures between 19 and 40 ka of ca. 13 °C and an increase of ca. 4 °C until 7 ka, after which it remained relatively stable (Fig. 1). The $\text{TEX}^{H_{86}}$ (from Varma et al., 2023) reveals temperatures between 10.3 and 15.9 °C and a similar increase in increasing trend of 4.5 °C from 20 ka till ca. 1 ka. Thus, both proxies indicate a LGM to recent temperature change of ca. 4 °C, consistent 225 with SST proxy records from ODP core 1234 which also showed a temperature change of 4 °C from 20 ka till ca. 1 ka for both $\text{TEX}^{H_{86}}$ and $U_{37}^{K'}$ respectively (de Bar et al., 2018).

Adkins et al. (2002, 2001) suggested a similar bottom water temperature change of 4 °C for the Pacific, Southern, and Atlantic deep oceans, and thus we assume a similar temperature change for the bottom water as reconstructed for the surface water. Combined with the $\delta^{18}\text{O}$ values of *Uvigerina* this translates to a negative $\delta^{18}\text{O}_{\text{BSW}}$ shift of 0.8 ± 0.2‰ (averaged values with

230 standard deviation of for ODP 1235 and 1234 and a temperature error of $\pm 1^{\circ}\text{C}$) from LGM to 1 ka using Eq. (6). This $\delta^{18}\text{O}_{\text{BSW}}$ shift subsequently translates, according to using the modern open-ocean $\delta^{18}\text{O}_{\text{sw}} - \delta^2\text{H}_{\text{sw}}$ relationship described in Eq. (1) and considering the error of the slope, to a $\delta^2\text{H}_{\text{BSW}}$ shift of ca. $-5.5 \pm 1.8\text{‰}$ for bottom waters (Table 1). This is similar to the values reported by Schrag et al. (2002), who measured oxygen and hydrogen isotopes of pore fluid from deep-sea sediments in the Southern and Northern Atlantic Ocean and observed a negative shift in $\Delta\delta^{18}\text{O}_{\text{BSW}}$ of $0.7 \pm 1.1\text{‰}$ and $\Delta\delta^2\text{H}_{\text{BSW}}$ of $6 \pm 9\text{‰}$ during
235 the last deglaciation.

3.2 Reconstruction of surface seawater isotopes based on alkenones

The $\delta^2\text{H}_{\text{C}37}$ values in core ODP 1235 range between -193‰ to -169‰ (Fig. 2). Between 40 ka and 25 ka the stable isotope ratio is relatively stable at ca. -180‰ , then increases to -169‰ and decreases again to -173‰ at the LGM (ca. 20 ka) and down to the more negative value of -193‰ in the most recent sample. This record compares well, both in trend as well as in absolute
240 values, with that of the previously published $\delta^2\text{H}_{\text{C}37}$ record of ODP 1234 (Weiss et al., 2019a; Fig. 2), confirming that the trends in $\delta^2\text{H}_{\text{C}37}$ happened on a regional scale. If we calculate the overall shift from the LGM (21 ka) to the most recent sample, then both records show a shift in $\delta^2\text{H}_{\text{C}37}$ of $-20 \pm 3\text{‰}$ (error indicates replicate analysis error). Published $\delta^2\text{H}_{\text{C}37}$ alkenone records
245 from Late Quaternary sediment cores (Kasper et al., 2014; Pahnke et al., 2007; Petrick et al., 2015; Simon et al., 2015 and Weiss et al., 2019b) report $\delta^2\text{H}_{\text{C}37}$ shifts which are very similar in magnitude (see overview in Table 1) and average $-20 \pm 3.22 \pm 5\text{‰}$ for the last deglaciation. This suggests, indicating that this shift in hydrogen isotopic composition of C_{37} alkenones is globally surprisingly quite similar in magnitude for different oceans, despite the large differences in oceanographic settings. Since Mix et al. (2003) observed the dominance of the open-ocean species *E. huxleyi* coccoliths in ODP 1234 and Hagino et al. (2004, 2006) and Menschel et al. (2016) showed that the dominant alkenone producer on the west coast of South America
250 is the Group III haptophyte *E. huxleyi*, it is most likely that alkenones in both cores reflect an open-ocean Group III haptophyte signal. We can therefore apply the SPOM calibration of Gould et al. (2019) (Eq. 7) to estimate the hydrogen isotopic composition of the seawater from the $\delta^2\text{H}_{\text{C}37}$. The resulting record (Fig. 2) shows a $\delta^2\text{H}_{\text{SSW}}$ value of ca. 4‰ for the uppermost sample and ca. 18‰ for the LGM for ODP 1235 (Table 1). Conversion of the shift in $\delta^2\text{H}_{\text{C}37}$ of $-20 \pm 3\text{‰}$ into $\Delta\delta^2\text{H}_{\text{SSW}}$, using the calibration of Gould et al. (2019) and considering the error in the slope of that calibration, results in a shift of $-14 \pm 4\text{‰}$ from LGM to the most recent sample. Application of the core-top calibration from Mitsunaga et al. (2022) (Eq. 8) gives an
255 identical change of $-14 \pm 3\text{‰}$.

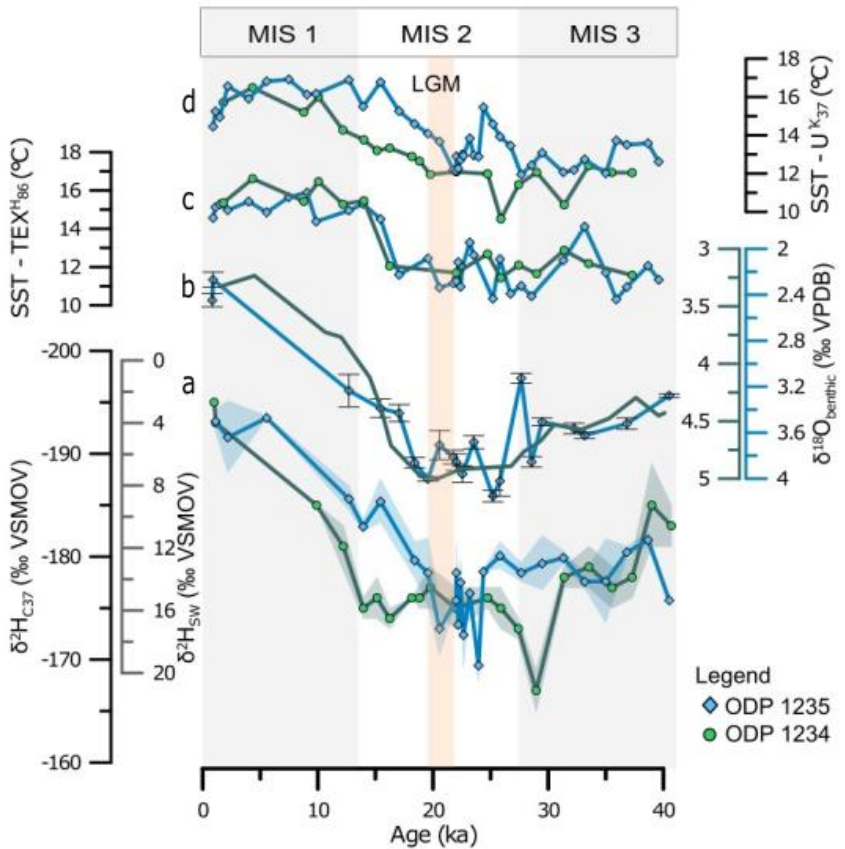


Figure 2: (a) Hydrogen isotope records of C_{37} alkenones of ODP 1235, blue diamonds and neighbouring ODP 1234 (Weiss et al., 2019), green circles, both from the Chilean Margin. The shading represents the standard deviation of duplicate isotope measurements. Also shown are δ^2H values of surface seawater calculated using Gould et al. (2019). (b) $\delta^{18}O$ of *Uvigerina* from ODP 1235 in blue with diamonds, error bars indicate standard deviation. The green line shows the 5pt average $\delta^{18}O$ of benthic foraminifera from ODP 1234 (from de Bar et al., 2019). Published organic proxy reconstructions are shown in (c) with TEX^{H}_{86} and (d) $U^{K'}_{37}$ index. SST data from ODP 1234 are from de Bar et al. (2019) – and from ODP 1235 from Varma et al. (2023 *under revision*).

3.3 Comparison of seawater isotopes and paleo salinity implications

The reconstructed $\Delta\delta^2H_{SSW}$ of ca. -14‰ from C_{37} alkenones is higher than that inferred from the benthic foraminifera isotopes (ca. $-5 \pm 4\text{‰}$) and measured in pore fluids (Schrag et al., 2002), implying that the isotopic composition of the sea surface water experienced a larger change during the last deglaciation compared to the bottom water isotope composition at the Chilean Margin. Potentially, we underestimated the change in the latter due to a lack of reconstructed bottom water temperatures. However, sensitivity analysis shows that even with much smaller bottom water temperature changes than used here, the magnitude of δ^2H_{BSW} change will still be lower than that of δ^2H_{SSW} . For example, in the unlikely scenario that bottom water temperatures have remained constant, the maximum change of $\Delta\delta^{18}O_{BSW}$ is still only $-1.6 \pm 0.2\text{‰}$, or $-10.6 \pm 2\text{‰}$ of $\Delta\delta^2H_{BSW}$.

Thus, it seems likely that at the Chilean Margin the glacial–interglacial change in surface water isotopes was larger than that of bottom water isotopes. The large regional change in $\delta^2\text{H}_{\text{SSW}}$ could be due to changes in local climate resulting in increased precipitation and/or decreased evaporation or increased freshwater runoff, for instance. Both cores, ODP 1235 and ODP 1234, are located within the Chile–Peru upwelling system and near to two major river mouths Río Biobío and Río Itata, both draining large basins (Muratli et al., 2010a). However, de Bar et al. (2018) observed no major change in the contribution of terrestrially derived biomarker concentrations and in proxies for river transported material like the BIT index (Hopmans et al., 2016) and the C₃₂ 1,15-diol index (de Bar et al., 2016, Lattaud et al., 2017a, b).

To reconstruct salinity change we applied the modern open-ocean $\delta^2\text{H}_{\text{SW}}$ –salinity and $\delta^{18}\text{O}_{\text{SW}}$ –salinity relationships (Eq. 2 and 3; based on data from 0–300 meter depth). The bottom water $\Delta\delta^{18}\text{O}_{\text{BSW}}$ based on measured benthic foraminifera $\delta^{18}\text{O}$ values, translate using Eq. (3) and considering the error in the slope, to a change in bottom water salinity of 1 ± 0.2 psu, and are in line with earlier estimations based on oxygen isotopes and sea level reconstructions (e.g. Adkins et al., 2002; Duplessy et al., 2002; Oba et al., 2004; Waelbroeck et al., 2002). The $\Delta\delta^2\text{H}_{\text{SSW}}$ of ca. $\pm 14\text{‰}$, based on $\delta^2\text{H}_{\text{C37}}$, translates using Eq. (2) and considering the error in the slope, to a regional salinity change of ca. 3 ± 1 psu, a larger reconstructed change in salinity than for bottom waters, but similar to the estimate of Lamy et al. (2002) who reconstructed a sea surface paleosalinity shift from 36 to 33 psu during the last 8 ka based on $\delta^{18}\text{O}$ of planktic foraminifera for the southern Chilean Margin core ODP 1233. The observed freshening in the surface waters relative to bottom waters may be due to a stronger input in relatively low salinity waters from the Southern Ocean (ACC/PCC) and/or more transport of low salinity Chilean Fjord Water (CFW) that, as a result of higher temperatures and intensifying continental meltwater input, resulted in even lower salinity surface water at the study site.

3.4 Global distribution of hydrogen isotope changes during last deglaciation

To examine the global distribution of hydrogen isotopes during the last deglaciation we compare the two Chilean Margin records to published global alkenone hydrogen isotope records (Table 1). These comprise five low to mid-latitude records of which four show a negative glacial–interglacial shift while the record from the Mozambique Channel of Kasper et al. (2015) reflects a positive change. The latter may be due to the close location to the river mouth, with varying freshwater input during the last 20 kyrs, and therefore this record is not further considered here. If we calculate $\delta^2\text{H}_{\text{SSW}}$ from the remaining four published $\delta^2\text{H}_{\text{C37}}$ records and compare this to our record, we find a remarkably similar negative shift from LGM to Recent in the $\delta^2\text{H}_{\text{SSW}}$ between 11–17‰ for different parts of the globe (Table 1), suggesting there might be a global aspect to this relatively large negative glacial–interglacial shift in sea surface seawater hydrogen isotope composition. This shift is larger than the shift inferred for bottom seawaters, compared to the smaller shift observed in bottom waters (e.g. Schrag et al., 2002). There could be several reasons for this globally observed similar change in surface water hydrogen isotopic composition. For example, increasing average global temperatures during the deglaciation could have intensified the hydrological cycle leading to high precipitation rates and runoff (including meltwater) in many places across the globe, at least around South America and South Africa where most records originate from. This increased freshening of surface waters may have led to an additional depletion in ^2H compared to those of bottom waters. Furthermore, the salinity– ^2H relationship in surface waters might have

been different during the glacial compared to the interglacial due to a different evaporation-precipitation balance. Another reason could be a change in the global waterline between the glacial and interglacial, where the slope of the $\delta^2\text{H}$ - $\delta^{18}\text{O}$ relationship changed for the surface waters. Rohling et al., (2007) showed, for example, that the $\delta^{18}\text{O}$ - $\delta^2\text{H}$ relationship of the evaporative Mediterranean is significantly different from that of the modern open-ocean and demonstrated the influence of a dominating evaporation on the slope-isotope-salinity relationship. Indeed, Putman et al. (2019) suggested that hydroclimate processes are important controls on the slope and intercept of local meteoric water-lines. Surface waters may be more sensitive to changes in the $\delta^{18}\text{O}$ - $\delta^2\text{H}$ relationship due to their direct atmosphere connection in contrast to bottom waters. Surface waters may be more sensitive for changes in this salinity-hydrogen isotope relationship due to the direct atmosphere connection. Potentially there was a steeper salinity- $\delta^2\text{H}$ slope of Eq. (2) for surface waters, due to e.g. increased surface seawater evaporation during the LGM. This slope may have been changing during deglaciation towards the value and thus result in a large change in surface water $\delta^2\text{H}$ despite a similar shift in salinity as that in bottom waters.

To verify these assumptions, further application of $\delta^2\text{H}_{\text{C37}}$ analyses of sediment cores at different open-ocean locations and combined $\delta^{18}\text{O}$ foraminifera analyses or pore fluid oxygen and hydrogen isotope reconstructions (Schrag et al., 2002) are needed to study the past meteoric open-ocean waterline of surface and bottom waters. Extending our understanding of the (past) relationship of seawater isotopes and salinity could help to understand and reconstruct ocean current and ocean mixing processes.

320

Table 1: Comparison of the seawater isotope changes between the Last Glacial Maximum (21 ka) to Recent for different sediment cores. Calculated hydrogen isotopic composition of seawater is based on SPOM calibration (Gould et al., 2019) and sediment core top calibration (Mitsunaga et al., 2022). Oxygen isotopes of the bottom seawater are calculated with Cramer et al. (2011) and a temperature change estimate of 4 °C. For Petrick et al. (2015) a bottom water temperature change of 2 °C is estimated based on the SST data from that record.

Core	Location	Source	Recent				LGM				Difference LGM-Recent		
			Age (ka)	$\delta^2\text{H}_{\text{C37}}$ (‰)	$\delta^2\text{H}_{\text{SSW}}$ (‰)	$\delta^2\text{H}_{\text{SSW}}$ (‰)	Age (ka)	$\delta^2\text{H}_{\text{C37}}$ (‰)	$\delta^2\text{H}_{\text{SSW}}$ (‰)	$\delta^2\text{H}_{\text{SSW}}$ (‰)	$\Delta\delta^2\text{H}_{\text{C37}}$ (‰)	$\Delta\delta^2\text{H}_{\text{SSW}}$ (‰)	$\Delta\delta^2\text{H}_{\text{SSW}}$ (‰)
				SPOM	Core top		SPOM	Core top		SPOM	Core top		
JPC32	Panama Basin	Pahnke et al. (2007)	0.3	-221	-15	-20	21.1	-198	1	-4	-23	-16	-16
MD02-2594	Southern South Africa	Kasper et al. (2014)	3.5	-192	5	0	21.1	-173	18	13	-19	-13	-13
164PE304-80	Mozambique channel	Kasper et al. (2015)	0.8	-189	7	2	21.3	-196	2	-3	7	5	6
ODP 1087	Southwest Africa	Petrick et al. (2015)	2.7	-205	-4	-9	23.1	-180	13	8	-25	-17	-17
CD154 10-06P	Southeast Africa	Simon et al. (2015)	2	-195	3	-2	20.1	-179	14	9	-16	-11	-11
ODP 1234	Chilean Margin	Weiss et al. (2019)	1	-195	3	-2	20.1	-176	16	11	-19	-13	-13
ODP 1235	Chilean Margin	This study	1.1	-193	4	-1	20.6	-173	18	13	-20	-14	-14
				Age (ka)	$\delta^{18}\text{O}_{\text{foram}}$ (‰)			Age (ka)	$\delta^{18}\text{O}_{\text{foram}}$ (‰)		$\Delta\delta^{18}\text{O}_{\text{foram}}$ (‰)	$\Delta\delta^{18}\text{O}_{\text{BSW}}$ (‰)	$\Delta\delta^2\text{H}_{\text{BSW}}$ (‰)
ODP 1234	Chilean Margin	Weiss et al. (2019)	0.78	3.3			20.1	5			-1.7	-0.9	-6.2
ODP 1235	Chilean Margin	This study	0.9	2.3			20.56	3.8			-1.5	-0.7	-4.8
ODP 1087	Southwest Africa	Petrick et al. (2015)	1.6	2.7			21.1	4			-1.3	-0.9	-6.2
LR04 stack	Global	Lisicki and Raymo (2005)	0	3.2			20	5			-1.8	-1	-6.8

325

4 Conclusion

The ODP 1235 sediment record shows a ~~similar~~ large shift in $\delta^2\text{H}_{\text{C}37}$ during the last deglaciation at the Chilean Margin ~~similar to the as observation reported in~~ Weiss et al. (2019) for nearby core site ODP 1234, demonstrating that the shift is regionally consistent. The hydrogen isotope ratios of alkenones are thus a reproducible paleo proxy for relative changes in $\delta^2\text{H}_{\text{SSW}}$ and 330 likely suggests changes in the salinity of the surface water. The reconstructed ~~glacial-interglacial~~ change in ~~the~~ hydrogen ~~isotopes isotopic composition of surface sea-water is ca. -14‰, independent of calibration using either the Gould et al. (2019) or Mitsunaga et al. (2022) calibration.~~ In contrast, the change in hydrogen isotopic composition of the bottom ~~sea~~ water reconstructed with the oxygen isotopic signature of benthic foraminifera was only ~~ca. $\Delta\delta^2\text{H} = -5\pm 1\text{‰}$. This indicates a larger change of the salt content in the surface water than the bottom water. Published Globally distributed C_{37} alkenone records~~ 335 ~~from other oceans reveal a similarly large $\delta^2\text{H}_{\text{SW}}$ change, for the surface waters than bottom water isotopes reconstructed from benthic foraminifera and suggest globally more freshening of surface waters compared to bottom waters. Possibly more freshening of the surface waters or a change in the slope of the modern $\delta^{18}\text{O}-\delta^2\text{H}$ open-ocean waterline of took place.~~ Further application of $\delta^2\text{H}_{\text{C}37}$ analyses combined with $\delta^{18}\text{O}$ foraminifera analyses or pore fluid oxygen and hydrogen isotope reconstructions may improve our ~~picture understanding~~ of the past ocean seawater isotopic composition and salinity changes 340 between surface and bottom water.

Data Availability

This study contains supplementary material. Supplement file 1 includes the age model and additional figures of the modern open-ocean salinity and isotope dataset used and cited in this study. Supplement file 2 contains the analysed isotope data of 345 ODP 1235. The age model, sea surface temperature and isotope dataset are archived at PANGAEA (Hättig et al., 2023a,b; Varma et al., 2023).

Sample availability

All processed sediment samples are stored at NIOZ, i.e. TLE, Apolar, Ketone, Polar fractions of ODP 1234 and ODP 1235 core and sieved material of ODP 1235.

Author contribution

350 All four (co-) authors collectively contributed to the conceptualisation of this study. Devika Varma and Katrin Hättig ordered samples from IODP and made sample splits for different analysis. Devika Varma prepared apolar, ketone and polar fractions and analysed ~~and integrated~~ alkenone and GDGTs for sea surface temperature. Katrin Hättig analysed the hydrogen isotopic composition of alkenones and performed the inorganic sample preparation, analysis, and age model computation.

Visualisation of research results and original draft preparation was done by Katrin Hättig. Stefan Schouten, Marcel T. J. van 355 der Meer and Devika Varma reviewed and edited the original draft.

Competing interests

The authors declare that they have no conflict of interest.

Acknowledgement

We thank Michelle Penkrot from IODP Gulf Coast Repository for providing samples of ODP site 1235. Jort Ossebaar, and 360 Ronald van Bommel and Piet van Gaever are thanked for analytical support. This work was carried out under the umbrella of the Netherlands Earth System Science Centre (NESSC). This project has received funding from the European Union's Horizon 2020 research and innovation programme under the Marie Skłodowska-Curie, grant agreement No 847504.

References

Adkins, J. and Schrag, D. P.: Pore fluid constraints on deep ocean temperature and salinity during the last glacial maximum, 365 American Geophysical Union, 28, 771–774, 2001.

Adkins, J. F., McIntyre, K., and Schrag, D. P.: The salinity, temperature, and $\delta^{18}\text{O}$ of the glacial deep ocean, *Science*, 298, 1769–1773, <https://doi.org/10.1126/science.1076252>, 2002.

Bakun, A.: Global Climate Change and Intensification of Coastal Ocean Upwelling, *Science*, 892, 1989

De Bar, M. W., Stolwijk, D. J., McManus, J. F., Sinnenhe Damsté, J. S., and Schouten, S.: A late Quaternary climate record 370 based on long-chain diol proxies from the Chilean margin, *Clim. Past*, <https://doi.org/10.5194/cp-14-1783-2018>, 2018.

Bemis, B. E., Spero, H. J., Bijma, J., and Lea, D. W.: Reevaluation of the oxygen isotopic composition of planktonic foraminifera: Experimental results and revised paleotemperature equations, *Paleoceanography*, 13, 150–160, <https://doi.org/10.1029/98PA00070>, 1998.

Billups, K. and Schrag, D. P.: Paleotemperatures and ice volume of the past 27 Myr revisited with paired Mg/Ca and 375 $^{18}\text{O}/^{16}\text{O}$ measurements on benthic foraminifera, *Paleoceanography*, 17, <https://doi.org/10.1029/2000pa000567>, 2002.

Billups, K. and Schrag, D. P.: Application of benthic foraminiferal Mg/Ca ratios to questions of Cenozoic climate change, *Earth Planet. Sci. Lett.*, 209, 181–195, [https://doi.org/10.1016/S0012-821X\(03\)00067-0](https://doi.org/10.1016/S0012-821X(03)00067-0), 2003.

Blaauw, M. and Christeny, J. A.: Flexible paleoclimate age-depth models using an autoregressive gamma process, *Bayesian 380 Anal.*, 6, 457–474, <https://doi.org/10.1214/11-BA618>, 2011.

Broecker, W. S. and Comer, G.: The Glacial World according to Wally, Eldigio Press, 2002.

Brassell, S., Eglington, G., Marlowe, I.: Molecular stratigraphy: a new tool for climatic assessment, *Nature*, 129–133, <https://doi.org/https://doi.org/10.1038/320129a0>, 1986.

385 Chivall, D., M'Boule, D., Sinke-Schoen, D., Sinninghe Damsté, J. S., Schouten, S., van der Meer, M. T. J.: The effects of growth phase and salinity on the hydrogen isotopic composition of alkenones produced by coastal haptophyte algae, *Geochim. Cosmochim. Acta*, 140, 381–390, <https://doi.org/https://doi.org/10.1016/j.gca.2014.05.043>, 2014.

Craig, H.: Isotopic Variations in Meteoric Waters, *Science*, 133, 1702–1703, <https://doi.org/10.1126/science.133.3465.1702>, 1961.

390 Craig, H. and Gordon, L. I.: Deuterium and oxygen 18 variations in the ocean and marine atmosphere, *Proc. Stable Isot. Oceanogr. Stud. Paleotemp. E. Tongiogi Ed.*, Spoleto, 1965.

Cramer, B. S., Toggweiler, J. R., Wright, J. D., Katz, M. E., and Miller, K. G.: Ocean overturning since the Late Cretaceous: Inferences from a new benthic foraminiferal isotope compilation, *Paleoceanography*, 24, <https://doi.org/10.1029/2008PA001683>, 2009.

395 Cramer, B. S., Miller, K. G., Barrett, P. J., and Wright, J. D.: Late Cretaceous-Neogene trends in deep ocean temperature and continental ice volume: Reconciling records of benthic foraminiferal geochemistry ($\delta^{18}\text{O}$ and Mg/Ca) with sea level history, *J. Geophys. Res. Ocean.*, 116, <https://doi.org/10.1029/2011JC007255>, 2011.

Cramer, F.: Scientific colour maps (8.0.0). Zenodo. <http://doi.org/10.5281/zenodo.5501399>, 2023

Duplessy, J. C., Labeyrie, L., Juillet-Leclerc, A., Maitre, F., Duprat, J., and Sarnthein, M.: Surface salinity reconstruction of 400 the North Atlantic Ocean during the Last Glacial maximum, *Oceanol. Acta*, 14, 311–324, 1991.

Duplessy, J. C., Labeyrie, L., and Waelbroeck, C.: Constraints on the ocean oxygen isotopic enrichment between the last glacial maximum and the holocene: Paleoceanographic implications, *Quat. Sci. Rev.*, 21, 315–330, [https://doi.org/10.1016/S0277-3791\(01\)00107-X](https://doi.org/10.1016/S0277-3791(01)00107-X), 2002.

Epstein, S., Buchsbaum, R., Lowenstam, H. A., and Urey, H. C.: Revised Carbonate-Water Isotopic Temperature Scale, 405 *GSA Bull.*, 64, 1315–1326, <https://doi.org/10.1130/0016-7606>, 1953.

Ganssen, G. M., Peeters, F. J. C., Metcalfe, B., Anand, P., Jung, S. J. A., Kroon, D., and Brummer, G. J. A.: Quantifying sea surface temperature ranges of the Arabian Sea for the past 20 000 years, *Clim. Past*, 7, 1337–1349, <https://doi.org/10.5194/cp-7-1337-2011>, 2011.

Gould, J., Kienast, M., Dowd, M., and Schefuß, E.: An open-ocean assessment of alkenone δD as a paleo-salinity proxy, 410 *Geochim. Cosmochim. Acta*, 246, 478–497, <https://doi.org/10.1016/j.gca.2018.12.004>, 2019.

Hättig, K.; Varma, D.; van der Meer, M. T. J.; Reichart, G.-J.; Schouten, S. (2023a): Age model for ODP Leg 202 Site 1235 and Site 1234. PANGAEA, <https://doi.org/10.1594/PANGAEA.957070>

Hättig, K.; Varma, D.; van der Meer, M. T. J.; Schouten, S. (2023b): Hydrogen isotopic composition of alkenones and oxygen isotopes of benthic foraminifera from ODP Site 202-1235. 415 PANGAEA, <https://doi.org/10.1594/PANGAEA.958880>

Häggi, C., Chiessi, C. M., and Schefuß, E.: Testing the D/H ratio of alkenones and palmitic acid as salinity proxies in the Amazon Plume, *Biogeosciences*, 12, 7239–7249, <https://doi.org/10.5194/bg-12-7239-2015>, 2015.

Hagino, K. and Okada, H.: Floral response of coccolithophores to progressive oligotrophication in the South Equatorial Current, *Pacific Ocean, Glob. Environ. Chang. Ocean L.*, 121–132, 2004.

420 Hagino, K. and Okada, H.: Intra- and infra-specific morphological variation in selected coccolithophore species in the equatorial and subequatorial Pacific Ocean, *Mar. Micropaleontol.*, 58, 184–206, <https://doi.org/10.1016/j.marmicro.2005.11.001>, 2006.

Hut, G.: Consultants' group meeting on stable isotope reference samples for geochemical and hydrological investigations, *Int. At. Energy Agency*, 49, 1987.

425 Kasper, S., Van Der Meer, M. T. J., Mets, A., Zahn, R., Sinninghe Damsté, J. S., and Schouten, S.: Salinity changes in the Agulhas leakage area recorded by stable hydrogen isotopes of C37 alkenones during Termination i and II, *Clim. Past*, 10, 251–260, <https://doi.org/10.5194/cp-10-251-2014>, 2014

Lamy, F., Rühlemann, C., Hebbeln, D., and Wefer, G.: High- and low-latitude climate control on the position of the southern Peru-Chile Current during the Holocene, *Paleoceanography*, 17, 16-1–16–10,

430 <https://doi.org/10.1029/2001pa000727>, 2002.

Lear, C. H., Wilson, P. A., Shackleton, N. J., and Elderfield, H.: Palaeotemperature and ocean chemistry records for the Palaeogene from Mg/Ca and Sr/Ca in benthic foraminiferal calcite, *GFF*, 122, 93, <https://doi.org/10.1080/11035890001221093>, 2000.

435 Lear, C. H., Rosenthal, Y., Coxall, H. K., and Wilson, P. A.: Late Eocene to early Miocene ice sheet dynamics and the global carbon cycle, *Paleoceanography*, 19, 1–11, <https://doi.org/10.1029/2004PA001039>, 2004.

Lear, C. H., Coxall, H. K., Foster, G. L., Lunt, D. J., Mawbey, E. M., Rosenthal, Y., Sosdian, S. M., Thomas, E., and Wilson, P. A.: Mg/Ca Paleothermometry Cross-References, *Paleoceanography*, 2004–2006, <https://doi.org/10.1002/2015PA002833>, 2015.

LeGrande, A. N. and Schmidt, G. A.: Global gridded data set of the oxygen isotopic composition in seawater, *Geophys. Res. Lett.*, 33, 1–5, <https://doi.org/10.1029/2006GL026011>, 2006.

Lynch-Stieglitz, J., Curry, W. B., and Slowey, N.: A geostrophic transport estimate for the Florida Current from the oxygen isotope composition of benthic foraminifera, *Paleoceanography*, 14, 360–373, <https://doi.org/10.1029/1999PA900001>, 1999.

440 M'boule, D., Chivall, D., Sinke-Schoen, D., Sinninghe Damsté, J., Schouten, S., and van der Meer, M. T. J.: Salinity dependent hydrogen isotope fractionation in alkenones produced by coastal and open ocean haptophyte algae, *Geochim. Cosmochim. Acta*, 130, 126–135, <https://doi.org/https://doi.org/10.1016/j.gca.2014.01.029>, 2014a.

M'boule, D., Chivall, D., Sinke-Schoen, D., Sinninghe Damsté, J. S., Schouten, S., and Van der Meer, M. T. J.: Salinity dependent hydrogen isotope fractionation in alkenones produced by coastal and open ocean haptophyte algae, *Geochim. Cosmochim. Acta*, 130, 126–135, <https://doi.org/10.1016/j.gca.2014.01.029>, 2014b.

450 Martin, P. A. and Lea, D. W.: A simple evaluation of cleaning procedures on fossil benthic foraminiferal Mg/Ca, *Geochemistry, Geophys. Geosystems*, 3, <https://doi.org/10.1029/2001GC000280>, 2002.

McCrea, J. M.: On the Isotopic Chemistry of Carbonates and a Paleotemperature Scale, *J. Chem. Phys.*, 18, 849–857, <https://doi.org/10.1063/1.1747785>, 1950.

van der Meer, M. T. J., Benthien, A., French, K. L., Epping, E., Zondervan, I., Reichart, G. J., Bijma, J., Sinninghe Damsté, J. S., and Schouten, S.: Large effect of irradiance on hydrogen isotope fractionation of alkenones in *Emiliania huxleyi*, *Geochim. Cosmochim. Acta*, 160, 16–24, <https://doi.org/10.1016/j.gca.2015.03.024>, 2015.

455 Van der Meer, M. T. J., Benthien, A., Bijma, J., Schouten, S., and Sinninghe Damsté, J. S.: Alkenone distribution impacts the hydrogen isotopic composition of the c37:2 and c37:3 alkan-2-ones in *emiliania huxleyi*, *Geochim. Cosmochim. Acta*, 111, 162–166, <https://doi.org/10.1016/j.gca.2012.10.041>, 2013.

460 Menschel, E., González, H. E., and Giesecke, R.: Coastal-oceanic distribution gradient of coccolithophores and their role in the carbonate flux of the upwelling system off Concepción, Chile (36°S), *J. Plankton Res.*, 38, 798–817, <https://doi.org/10.1093/plankt/fbw037>, 2016.

Mitsunaga, B. A., Novak, J., Zhao, X., Dillon, J. A., Huang, Y., and Herbert, T. D.: Alkenone $\delta^{2\text{H}}$ values – a viable sea water isotope proxy? New core-top $\delta^{2\text{H}}\text{C}37:3$ and $\delta^{2\text{H}}\text{C}37:2$ data suggest inter-alkenone and alkenone-water hydrogen 465 isotope fractionation are independent of temperature and salinity, *Geochim. Cosmochim. Acta*, 339, 139–156, <https://doi.org/10.1016/j.gca.2022.10.024>, 2022.

Mix, A., Tiedemann, R., and Blum, P.: Proceedings of the Ocean Drilling Program, Vol. 202. Initial Reports. Southeast Pacific Paleoceanographic Transects, *Ocean Drill. Progr.*, 2003a.

Mix, A. C., Tiedemann, R., Blum, P., and Scientists, S.: LEG 202 SUMMARY, Proc. ODP, Initial Reports, 202 Coll. 470 Station. TX (Ocean Drill. Program), 202, 1–145, 2003b.

Mulitza, S., Boltovskoy, D., Donner, B., Meggers, H., Paul, A., and Wefer, G.: Temperature: $\delta^{18\text{O}}$ relationships of planktonic foraminifera collected from surface waters, *Palaeogeogr. Palaeoclimatol. Palaeoecol.*, 202, 143–152, [https://doi.org/10.1016/S0031-0182\(03\)00633-3](https://doi.org/10.1016/S0031-0182(03)00633-3), 2003.

Muratli, J. M., Chase, Z., Mix, A. C., and McManus, J.: Increased glacial-age ventilation of the Chilean margin by Antarctic 475 Intermediate Water, *Nat. Geosci.*, 3, 23–26, <https://doi.org/10.1038/ngeo715>, 2010.

O’Neil, J. R., Clayton, R. N., and Mayeda, T. K.: Oxygen Isotope Fractionation in Divalent Metal Carbonates, *J. Chem. Phys.*, 51, 5547–5558, <https://doi.org/10.1063/1.1671982>, 1969.

Oba, T. and Murayama, M.: Sea-surface temperature and salinity changes in the northwest Pacific since the last glacial maximum, *J. Quat. Sci.*, 19, 335–346, <https://doi.org/10.1002/jqs.843>, 2004.

480 Pahnke, K., Sachs, J. P., Keigwin, L., Timmermann, A., and Xie, S. P.: Eastern tropical Pacific hydrologic changes during the past 27,000 years from D/H ratios in alkenones, *Paleoceanography*, 22, 1–15, <https://doi.org/10.1029/2007PA001468>, 2007.

Pearson, P. N.: Oxygen Isotopes in Foraminifera: Overview and Historical Review, *Paleontol. Soc. Pap.*, 18, 1–38,

https://doi.org/10.1017/s1089332600002539, 2012.

485 Petersen, S. V. and Schrag, D. P.: Antarctic ice growth before and after the Eocene-Oligocene transition: New estimates from clumped isotope paleothermometry, *Paleoceanography*, 30, 1305–1317, https://doi.org/10.1002/2014PA002769, 2015.

Petrick, B. F., McClymont, E. L., Marret, F., and Van Der Meer, M. T. J.: Changing surface water conditions for the last 500ka in the Southeast Atlantic: Implications for variable influences of Agulhas leakage and Benguela upwelling, 490 *Paleoceanography*, 30, 1153–1167, https://doi.org/10.1002/2015PA002787, 2015.

Prahl, F. G. and Wakeham, S. G.: Calibration of unsaturation patterns in long-chain ketone compositions for palaeotemperature assessment, *Nature*, 330, 367–369, https://doi.org/10.1038/330367a0, 1987.

Putman, A. L., Fiorella, R. P., Bowen, G. J., and Cai, Z.: A Global Perspective on Local Meteoric Water Lines: Meta - analytic Insight Into Fundamental Controls and Practical Constraints, *Water Resour. Res.*, 55, 6896–6910, 495 https://doi.org/10.1029/2019WR025181, 2019.

Reimer, P. J., Baillie, M. G. L., Bard, E., Bayliss, A., Beck, J. W., Blackwell, P. G., Bronk Ramsey, C., Buck, C. E., Burr, G. S., Edwards, R. L., Friedrich, M., Grootes, P. M., Guilderson, T. P., Hajdas, I., Heaton, T. J., Hogg, A. G., Hughen, K. A., Kaiser, K. F., Kromer, B., McCormac, F. G., Manning, S. W., Reimer, R. W., Richards, D. A., Southon, J. R., Talamo, S., Turney, C. S. M., van der Plicht, J., and Weyhenmeyer, C. E.: IntCal09 and Marine09 Radiocarbon 500 Age Calibration Curves, 0–50,000 Years cal BP, *Radiocarbon*, 51, 1111–1150, https://doi.org/10.1017/S0033822200034202, 2009.

Rohling, E. J.: Progress in paleosalinity: Overview and presentation of a new approach, *Paleoceanography*, 22, 1–9, https://doi.org/10.1029/2007PA001437, 2007.

Rohling, E. J. and Bigg, G. R.: Paleosalinity and $\delta^{18}\text{O}$: A critical assessment , *J. Geophys. Res. Ocean.*, 103, 1307–1318, 505 https://doi.org/10.1029/97jc01047, 1998.

Rohling, E. J. and Cooke, S.: Stable oxygen and carbon isotopes in foraminiferal carbonate shells, in: *Modern Foraminifera*, Springer Netherlands, Dordrecht, 239–258, https://doi.org/10.1007/0-306-48104-9_14, 1999.

Rostek, F., Ruhlandt, G., Bassinot, F. C., Muller, P. J., Labeyrie, L. D., Lancelot, Y., and Bard, E.: Reconstructing sea 510 surface temperature and salinity using $\delta^{18}\text{O}$ and alkenone records, *Nature*, 364, 319–321, https://doi.org/10.1038/364319a0, 1993.

Rostek, F., Bard, E., Beaufort, L., Sonzogni, C., and Ganssen, G.: Sea surface temperature and productivity records for the last 240 kyr on the Arabian Sea, *Deep. Res. Part II Top. Stud. Oceanogr.*, 44, 1461–1480, https://doi.org/10.1016/S0967-0645(97)00008-8, 1997.

Sachs, J. P. and Kawka, O. E.: The influence of growth rate on 2H/1H fractionation in continuous cultures of the 515 coccolithophorid *Emiliania huxleyi* and the diatom *Thalassiosira pseudonana*, *PLoS One*, 10, https://doi.org/10.1371/journal.pone.0141643, 2015.

Sachs, J. P., Maloney, A. E., Gregersen, J., and Paschall, C.: Effect of salinity on 2H/1H fractionation in lipids from

continuous cultures of the coccolithophorid *Emiliania huxleyi*, *Geochim. Cosmochim. Acta*, 189, 96–109, <https://doi.org/https://doi.org/10.1016/j.gca.2016.05.041>, 2016.

520 Schouten, S., Hopmans, E. C., Schefuß, E., and Sinninghe Damsté, J. S.: Corrigendum to “Distributional variations in marine crenarchaeotal membrane lipids: a new tool for reconstructing ancient sea water temperatures?,” *Earth Planet. Sci. Lett.*, 211, 205–206, [https://doi.org/10.1016/s0012-821x\(03\)00193-6](https://doi.org/10.1016/s0012-821x(03)00193-6), 2003.

Schouten, S., Ossebaar, J., Schreiber, K., Kienhuis, M. V. M., Langer, G., Benthien, A., and Bijma, J.: The effect of temperature, salinity and growth rate on the stable hydrogen isotopic composition of long chain alkenones produced by *Emiliania huxleyi* and *Gephyrocapsa oceanica*, *Biogeosciences*, 3, 113–119, <https://doi.org/10.5194/bg-3-113-2006>, 2006.

525 Schrag, D. P., Adkins, J. F., McIntyre, K., Alexander, J. L., Hodell, D. A., Charles, C. D., and McManus, J. F.: The oxygen isotopic composition of seawater during the Last Glacial Maximum, *Quat. Sci. Rev.*, 21, 331–342, [https://doi.org/https://doi.org/10.1016/S0277-3791\(01\)00110-X](https://doi.org/https://doi.org/10.1016/S0277-3791(01)00110-X), 2002.

530 Shackleton, N. J.: Attainment of isotopic equilibrium between ocean water and the benthonic foraminifera genus *Uvigerina*: Isotopic changes in the ocean during the last glacial, *Colloq. Int. du C.N.R.S.*, 219, 203–210, 1974.

Simon, M. H., Gong, X., Hall, I. R., Ziegler, M., Barker, S., Knorr, G., Van Der Meer, M. T. J., Kasper, S., and Schouten, S.: Salt exchange in the Indian-Atlantic Ocean Gateway since the Last Glacial Maximum: A compensating effect between Agulhas Current changes and salinity variations?, *Paleoceanography*, 30, 1318–1327, <https://doi.org/10.1002/2015PA002842>, 2015.

535 Spero, H. J., Bijma, J., Lea, D. W., and Bemis, B. E.: Effect of seawater carbonate concentration on foraminiferal carbon and oxygen isotopes, *Lett. to Nat.*, 390, 497–500, 1997.

Spero, H. J., Mielke, K. M., Kalve, E. M., Lea, D. W., and Pak, D. K.: Multispecies approach to reconstructing eastern equatorial Pacific thermocline hydrography during the past 360 kyr, *Paleoceanography*, 18, <https://doi.org/10.1029/2002PA000814>, 2003.

540 Srivastava, R., Ramesh, R., Jani, R. A., Anilkumar, N., and Sudhakar, M.: Stable oxygen, hydrogen isotope ratios and salinity variations of the surface Southern Indian Ocean waters, *Curr. Sci.*, 99, 1395–1399, 2010.

Strub, P. T., Mesías, M. J., Montecino, V., Rutllant, J., and Salinas, S.: Coastal ocean circulation off western South America coastal segment, 1998.

545 Tang, C. M. and Stott, L. D.: provide insight into the dynamics of monsoon In this study , we analyzed the stable isotopic composition of individual planktonic foraminifera after sapropel formation . Because individual single foraminiferal tests to the investigation of salinity change, 8, 473–493, 1993.

Varma, D.; Hättig, K.; van der Meer, M. .T J.; Reichart, G.-J.; Schouten, S. (2023a): SST Proxies Chilean (ODP Leg 202 Site 1235 and Site 1234) and Angola Margin (ODP Leg 175 Site 1078 and Site 1079).

550 PANGAEA, <https://doi.org/10.1594/PANGAEA.957090>

~~Varma, D.; Hättig, K.; van der Meer, M. .T J.; Reichart, G. J.; Schouten, S. (2023b): Constraining Water Depth Influence on~~

Varma, D., Hättig, K., van der Meer, M. T. J., Reichart, G. J., and Schouten, S.: Constraining Water Depth Influence on

Organic Paleotemperature Proxies Using Sedimentary Archives, Paleoceanogr. Paleoclimatology, 38,
<https://doi.org/10.1029/2022PA004533>, 2023.

555 Waelbroeck, C., Labeyrie, L., Michel, E., Duplessy, J. C., McManus, J. F., Lambeck, K., Balbon, E., and Labracherie, M.:
Sea-level and deep water temperature changes derived from benthic foraminifera isotopic records, Quat. Sci. Rev.,
21, 295–305, [https://doi.org/10.1016/S0277-3791\(01\)00101-9](https://doi.org/10.1016/S0277-3791(01)00101-9), 2002.

Weiss, G. M., Schouten, S., Sinninghe Damsté, J. S., and van der Meer, M. T. J.: Constraining the application of hydrogen
560 isotopic composition of alkenones as a salinity proxy using marine surface sediments, Geochim. Cosmochim. Acta,
250, 34–48, <https://doi.org/10.1016/j.gca.2019.01.038>, 2019a.

Weiss, G. M., Schouten, S., Sinninghe Damsté, J. S., and van der Meer, M. T. J.: Constraining the application of hydrogen
isotopic composition of alkenones as a salinity proxy using marine surface sediments, Geochim. Cosmochim. Acta,
250, 34–48, <https://doi.org/10.1016/j.gca.2019.01.038>, 2019b.

565 Weiss, G. M., de Bar, M. W., Stolwijk, D. J., Schouten, S., Sinninghe Damsté, J. S., and van der Meer, M. T. J.:
Paleosensitivity of Hydrogen Isotope Ratios of Long-Chain Alkenones to Salinity Changes at the Chile Margin,
Paleoceanogr. Paleoclimatology, 34, 978–989, <https://doi.org/10.1029/2019PA003591>, 2019c.

Weiss, G. M., Pfannerstill, Y. E., Schouten, S., Sinninghe Damsté, S. J., and van der Meer, T. J. M.: Effects of alkalinity and
salinity at low and high light intensity on hydrogen isotope fractionation of long-chain alkenones produced by
570 *Emiliania huxleyi*, Biogeosciences, 14, 5693–5704, <https://doi.org/10.5194/bg-14-5693-2017>, 2017.

Zhang, X., Gillespie, A. L., and Sessions, A. L.: Large D/H variations in bacterial lipids reflect central metabolic pathways,
Proc. Natl. Acad. Sci. U. S. A., 106, 12580–12586, <https://doi.org/10.1073/pnas.0903030106>, 2009.

Zhang, Z. and Sachs, J. P.: Hydrogen isotope fractionation in freshwater algae: I. Variations among lipids and species, Org.
Geochem., 38, 582–608, [https://doi.org/https://doi.org/10.1016/j.orggeochem.2006.12.004](https://doi.org/10.1016/j.orggeochem.2006.12.004), 2007.

575 Zweng, M. M., J. R. Reagan, D. Seidov, T. P. Boyer, R. A. Locarnini, H. E. Garcia, A. V. Mishonov, O. K. Baranova, K.
Weathers, C. R. P. and Smolyar, I.: World Ocean Atlas 2018, 2:Salinity, 82, 50, 2018